Contribution from the Department of Chemistry and Biochemistry, University of Maryland, College Park, Maryland 20742, and Department of Chemistry, University of Delaware, Newark, Delaware 19716

Synthesis, Molecular and Electronic Structure, and Properties of Mononuclear Trimethylphosphine-Containing Cyclopentadienyl Derivatives of Molybdenum(III) and Molybdenum(IV). Direct Evidence of Mo(III)–P π Back-Bonding

Steven T. Krueger,[1a] Rinaldo Poli,*,[1a] Arnold L. Rheingold,[1b] and Donna L. Staley[1b]

The compounds $MoCpX_2(PMe_3)_2$ [$Cp = \eta^5\text{-}C_5H_5$; X = Cl (**1**), Br (**2**), I (**3**)] have been prepared by interaction of $MoX_3(PMe_3)_3$ with TlCp in toluene or tetrahydrofuran. This reaction also generates as byproducts the Mo(II) species $Mo_2X_4(PMe_3)_4$ and $MoX_2(PMe_3)_4$. The latter have been isolated for X = Cl (**4**) and Br (**5**). Compounds **1–3** are paramagnetic, low-spin ($S = \frac{1}{2}$), mononuclear 17-electron compounds. The EPR spectra show hyperfine coupling to the molybdenum and phosphorus nuclei. Crystal structure data are as follows. Compound **1**: monoclinic, space group $P2_1/a$, $a = 12.536$ (2) Å, $b = 10.169$ (2) Å, $c = 13.071$ (1) Å, $\beta = 93.68$ (1)°, $V = 1663$ (1) Å^3, $Z = 4$, $d_c = 1.53$ g·cm^{-3}, $\mu(\text{Cu K}\alpha) = 112.90$ cm^{-1}, $R = 0.041$ ($R_w = 0.057$) for 145 parameters and 1805 observations with $F_o^2 > 3\sigma(F_o^2)$. Compound **3**: orthorhombic, space group $Pnma$, $a = 12.530$ (3) Å, $b = 11.212$ (3) Å, $c = 13.157$ (3) Å, $V = 1848.4$ (9) Å^3, $Z = 4$, $d_c = 2.04$ g·cm^{-3}, $\mu(\text{Mo K}\alpha) = 41.52$ cm^{-1}, $R = 0.0395$ ($R_w = 0.0443$) for 119 parameters and 1666 observations with $F_o > 5\sigma(F_o)$. Compound **5**: tetragonal, space group $I42m$, $a = 9.670$ (3) Å, $c = 12.281$ (3) Å, $V = 1148.5$ (6) Å^3, $Z = 2$, $d_c = 1.44$ g·cm^{-3}, $\mu(\text{Mo K}\alpha) = 42.71$ cm^{-1}, $R = 0.0251$ ($R_w = 0.0261$) for 81 parameters and 884 observations with $F_o > 5\sigma(F_o)$. The structure of compounds **1** and **3** is a typical four-legged piano stool with the Cp ring in a η^5 geometry that is slightly distorted toward η^3,η^2. The Mo–P distances are shorter than the usual separation between Mo(III) and phosphines. Compounds **1–3** have been studied electrochemically. They do not show an easy reduction to 18-electron Mo(II) species. On the other hand, they exhibit an easily accessible and reversible one-electron oxidation. A chemical oxidation of compound **1** has been accomplished with $AgPF_6$, and the 16-electron oxidation product $[MoCpCl_2(PMe_3)_2]PF_6$ (**6**) has been isolated and characterized. It is paramagnetic with two unpaired electrons. Crystal data: monoclinic, space group $P2_1/c$, $a = 7.0418$ (6) Å, $b = 19.985$ (2) Å, $c = 14.732$ (2) Å, $\beta = 95.86$ (1)°, $V = 2062.4$ (7) Å^3, $Z = 4$, $d_c = 1.70$ g·cm^{-3}, $\mu(\text{Cu K}\alpha) = 104.43$ cm^{-1}, $R = 0.055$ ($R_w = 0.067$) for 202 parameters and 1850 observations with $F_o^2 > 3\sigma(F_o^2)$. The geometry of the cation of compound **6** is identical with that of compound **1**. The Mo–Cl bond lengths decrease whereas the Mo–P bond lengths increase on going from **1** to **6**. This suggests the presence of Mo(III)–P π back-bonding. Fenske–Hall MO calculations have been performed on model compounds of **1** and **3**. The results of these calculations rationalize the bonding and magnetic and electrochemical properties of the compounds.

Introduction

As part of our interest in the chemical reactivity of transition-metal compounds where the metal has an odd-electron configuration, we started the investigation of molybdenum(III) cyclopentadienyl systems. The cyclopentadienyl ligand is known to stabilize kinetically its complexes and to increase the softness of the metal center, thereby increasing the ability of the metal to bind organic ligands. Only a few Mo(III)–Cp systems (Cp = η^5-C$_5$H$_5$) are known. These comprise dinuclear, diamagnetic, sulfido-bridged, metal–metal-bonded species of general formula $Mo_2Cp_2(\mu\text{-SR})_4^2$ and $[Mo_2Cp_2(\mu\text{-SMe})_3(CO)_2]X,^3$ the tetrachloro-bridged $Mo_2(\eta^5\text{-}C_5H_4R)_2(\mu\text{-Cl})_4,^{4a,b}$ and mononuclear phosphine adducts of the latter, that is $Mo(\eta^5\text{-}C_5H_4R)Cl_2L_2$ [L = PMe$_3$, PMe$_2$Ph; L$_2$ = bis(diisopropylphosphino)ethane].^{4a,b} A derivative with a fully methyl-substituted Cp ring, $Mo(\eta^5\text{-}C_5Me_5)Cl_2(PMe_3)_2$, has also been prepared.^{4c} The known diminished tendency of halide ions to bridge two metal centers with respect to the alkanethiolates accounts for the interaction of the tetrachloro-bridged species with phosphine donors to afford mononuclear, odd-electron derivatives.^{4} No such chemistry has been

described for the tetrakis(alkanethiolato)-bridged species. The halogenated Mo(III)–Cp derivatives were therefore the systems of our choice. We report here a synthetic method that allows the preparation of the complete series of compounds $MoCpX_2(PMe_3)_2$ with X = Cl, Br, and I, and a comprehensive study of their physicochemical properties, including molecular and electronic structure. The electrochemical properties have been investigated and the peculiar one-electron oxidation product is also described here.

Experimental Section

All operations were carried out under a dinitrogen atmosphere with carefully dried and distilled solvents by using standard Schlenk-line techniques. Instruments used were as follows: FTIR, Nicolet 5DXC; EPR, Bruker ER200; NMR, Bruker AF200; magnetic susceptibility balance, Johnson Matthey; UV/vis, Shimadzu UV-240; CV, EG&G 362. Elemental analyses were performed by Dr. F. Kasler, Chemistry Department, University of Maryland, by Galbraith Laboratories, Knoxville, TN, and by Midwest Microlab, Indianapolis, IN.

$MoX_3(PMe_3)_3$(X = Cl,^{5} I^6) and $MoBr_3(THF)_3^7$ were prepared according to procedures described in the literature. $MoBr_3(PMe_3)_3$ was prepared by an adaptation to the bromide system of the synthesis utilized for the chloride and iodide systems.^{5,6} PMe$_3$ (Aldrich) was trap-to-trap distilled prior to use.

Reaction of $MoX_3(PMe_3)_3$ (X = Cl, Br, I) with TlCp. Preparation of $MoCpX_2(PMe_3)_2$. (a) X = Cl. To a solution of $MoCl_3(PMe_3)_3$ in THF (25 mL), prepared in situ from $MoCl_3(THF)_3$ (1.35 g, 3.22 mmol) and PMe$_3$ (1.0 mL, 9.7 mmol) was added TlCp (0.87 g, 3.22 mmol). The mixture was refluxed for 2 days with UV/visible monitoring [$MoCl_3$-$(PMe_3)_3$ has bands at 397, 332, and 280 nm]. The resultant reaction mixture was filtered through Celite and the filtrate evaporated under reduced pressure. The residue was redissolved in toluene (ca. 15 mL). After filtration and concentration to ca. 5 mL, the solution was layered with *n*-heptane. A mixture of dark red crystals of $MoCpCl_2(PMe_3)_2$ (**1**) and a few yellow-orange crystals of $MoCl_2(PMe_3)_4$ (**4**) was obtained. Analytically pure samples were obtained by hand-picking. Anal. Calcd for C$_{11}$H$_{23}$Cl$_2$MoP$_2$: C, 34.4; H, 6.0. Found: C, 34.5; H, 6.0. Yield: 45%. IR (compound 1; Nujol mull, cm^{-1}): 1420 m, 1300 w, 1280 m,

(1) (a) University of Maryland. (b) University of Delaware.
(2) (a) King, R. B. *J. Am. Chem. Soc.* **1963**, *85*, 1587. (b) Connelly, N. G.; Dahl, L. F. *J. Am. Chem. Soc.* **1970**, *92*, 7470. (c) Rakowski DuBois, M.; Haltiwanger, R. C.; Miller, D. J.; Glatzmaier, G. *J. Am. Chem. Soc.* **1979**, *101*, 5245. (d) Rakowski DuBois, VanDerveer, M. C.; DuBois, D. L.; Haltiwanger, R. C.; Miller, W. K. *J. Am. Chem. Soc.* **1980**, *102*, 7456. (e) Rakowski DuBois, M. *J. Am. Chem. Soc.* **1983**, *105*, 3710. (f) McKenna, M.; Wright, L. L.; Miller, D. J.; Tanner, L.; Haltiwanger, R. C.; Rakowski DuBois, M. *J. Am. Chem. Soc.* **1983**, *105*, 5329. (g) Casewit, C. J.; Haltiwanger, R. C.; Noordik, J.; Rakowski DuBois, M. *Organometallics* **1985**, *4*, 119. (h) Casewit, C. J.; Rakowski DuBois, M. *J. Am. Chem. Soc.* **1986**, *108*, 5482. (i) Laurie, J. C. V.; Duncan, L.; Haltiwanger, R. C.; Weberg, R. T.; Rakowski DuBois, M. *J. Am. Chem. Soc.* **1986**, *108*, 6234. (j) Weberg, R. T.; Haltiwanger, R. C.; Laurie, J. C. V.; Rakowski DuBois, M. *J. Am. Chem. Soc.* **1986**, *108*, 6242.
(3) Gomes de Lima, M. B.; Guerchais, J. E.; Mercier, R.; Pétillon, F. Y. *Organometallics* **1986**, *5*, 1952.
(4) (a) Green, M. L. H.; Izquierdo, A.; Martin-Polo, J. J.; Mtetwa, V. S. B.; Prout, K. *J. Chem. Soc., Chem. Commun.* **1983**, 538. (b) Grebenik, P. D.; Green, M. L. H.; Izquierdo, A.; Mtetwa, V. S. B.; Prout, K. *J. Chem. Soc., Dalton Trans.* **1987**, 9. (c) Baker, R. T. Personal communication.

(5) Atwood, J. L.; Hunter, W. E.; Carmona-Guzman, E.; Wilkinson, G. *J. Chem. Soc., Dalton Trans.* **1980**, 467.
(6) Cotton, F. A.; Poli, R. *Inorg. Chem.* **1987**, *26*, 1514.
(7) Owens, B. E.; Poli, R.; Rheingold, A. L. *Inorg. Chem.* **1989**, *28*, 1456.

Table I. Selected Crystal Data for All Compounds

compd	1	3	5	6
formula	$C_{11}H_{23}Cl_2MoP_2$	$C_{11}H_{23}I_2MoP_2$	$C_{12}H_{36}Br_2MoP_4$	$C_{11}H_{23}Cl_2F_6MoP_3$
fw	384.10	567.05	560.15	529.06
space group	$P2_1/a$	$Pnma$	$I\bar{4}2m$	$P2_1/c$
a, Å	12.536 (2)	12.530 (3)	9.670 (3)	7.0418 (6)
b, Å	10.169 (2)	11.212 (3)	9.670 (3)	19.985 (2)
c, Å	13.071 (1)	13.157 (4)	12.281 (3)	14.732 (2)
α, deg	90	90	90	90
β, deg	93.68 (1)	90	90	95.86 (1)
γ, deg	90	90	90	90
V, Å^3	1663 (1)	1848.4 (9)	1148.5 (6)	2062.4 (7)
Z	4	4	2	4
d_c, g/cm^3	1.53	2.04	1.62	1.70
μ, cm^{-1}	112.90 (Cu Kα)	41.52 (Mo Kα)	42.71 (Mo Kα)	104.43 (Cu Kα)
radiation (monochromated in incident beam) (λ, Å)	Cu Kα (1.541 78)	Mo Kα (0.710 73)	Mo Kα (0.710 73)	Cu Kα (1.541 78)
temp, °C	20	23	23	20
transmissn factors: max, min	1.000, 0.525	0.071, 0.044	0.281, 0.238	1.000, 0.526
R^a	0.041	0.0395	0.0251	0.055
$R_w{}^b$	0.057	0.0443	0.0261	0.067

$^a R = \sum||F_o| - |F_c||/\sum|F_o|$. $^b R_w = [\sum w(|F_o| - |F_c|)^2/\sum w|F_o|^2]^{1/2}$; $w = 1/\sigma^2(|F_o|)$.

1275 m, 1100 w, 1020 w, 1000 w, 960 sh, 940 s, 850 w, 820 w, 790 w, 735 m, 670 w. $\mu_{eff} = 1.72$ μ_B. The EPR spectrum is shown in Figure 1a. The mother solution was blue and showed a visible absorption band at 580 nm. A single crystal of compound **1** for the X-ray analysis was obtained by recrystallization from toluene/n-heptane.

(b) X = Br. The reaction was carried out as described above for X = Cl, starting from MoBr$_3$(THF)$_3$ (1.19 g, 0.152 mmol), PMe$_3$ (0.67 mL, 6.46 mmol), and TlCp (0.62 g, 2.30 mmol), in 30 mL of THF. The reaction mixture was refluxed for ca. 2 days with UV/visible monitoring. Workup as described above yielded 0.53 g (52%) of MoCpBr$_2$(PMe$_3$)$_2$ (**2**). Anal. Calcd for C$_{11}$H$_{23}$Br$_2$MoP$_2$: C, 27.9; H, 4.9. Found: C, 27.4; H, 4.9. A few orange crystals of MoBr$_2$(PMe$_3$)$_4$ (**5**) were also obtained and separated from compound **2** by hand-picking. One of these was used for the X-ray analysis. IR (compound **2**, Nujol mull, cm^{-1}): 1420 m, 1295 m, 1275 m, 1105 w, 1110 w, 945 s, 845 w, ca. 815 sh, 795 w, 725 s, 665 w. $\mu_{eff} = 1.68$ μ_B. The EPR spectrum is shown in Figure 1b. IR (compound **5**, Nujol mull, cm^{-1}): 1435 m, 1420 m, 1410 m, 1290 m, 1275 m, 1265 m, 935 s, 850 m, 835 m, 725 m, 700 m, 655 m.

(c) X = I. A procedure similar to those described above for X = Cl, and Br gave a 33% yield of the product. A better yield was obtained by interacting MoI$_3$(PMe$_3$)$_3$ (0.73 g, 1.04 mmol) with TlCp (0.29 g, 1.07 mmol) in 20 mL of toluene at the reflux temperature for 1 day. After filtration, concentration to ca. 5 mL and layering with n-heptane (20 mL) gave a 60% yield of analytically pure product. Anal. Calcd for C$_{11}$H$_{23}$I$_2$MoP$_2$: C, 23.3; H, 4.1. Found: C, 23.7; H, 4.1. IR (Nujol mull, cm^{-1}): 1420 m, 1300 m, 1280 m, 1105 w, 1060 w, 1000 w, 950 s, 845 w, 840 w, 800 w m, 725 m, 670 w. $\mu_{eff} = 1.61$ μ_B. The EPR spectrum is shown in Figure 1c.

Reaction of Compound 1 with AgPF$_6$. Preparation of [MoCpCl$_2$-(PMe$_3$)$_2$]PF$_6$. Compound **1** (0.58 g, 1.51 mmol) was dissolved in 5 mL of dichloromethane. Addition of AgPF$_6$ (0.40 g, 1.60 mmol) caused the immediate precipitation of a dark precipitate, while the color of the solution turned to red-orange. After filtration, the solid was washed several times with dichloromethane until a colorless filtrate was obtained. The combined filtrated solutions were reduced in volume to ca. 10 mL, and 50 mL of n-heptane was added. The resulting red-orange microcrystalline precipitate was filtered out, washed with n-heptane, and dried under vacuum. Yield: 0.27 g (34%). Anal. Calcd for C$_{11}$H$_{23}$Cl$_2$F$_6$MoP$_3$: C, 25.0; H, 4.4; F, 21.6; P, 17.6. Found: C, 24.0; H, 4.3; F, 21.6; P, 18.2. IR (Nujol mull, cm^{-1}): 3110 w, 1430 w, 1415 w, 1300 w, 1285 m, 1020 w, 955 m, 870 m, 835 s, 825 s, 740 m, 670 w, 555 m, 520 w. UV/vis [CH$_2$Cl$_2$, room temperature, nm (ϵ/mol^{-1}·L·cm^{-1})]: 260 (>2000), 323 (935), 474 (1095).

A single crystal for the X-ray analysis was obtained by diffusion of ether into a dichloromethane solution of the compound.

X-ray Crystallography. (a) MoCpCl$_2$(PMe$_3$)$_2$ (1). A single crystal was glued to the inside of a thin-walled capillary, which was subsequently sealed under nitrogen and mounted on the diffractometer. Crystal data are assembled in Table I. The data reduction and the structure solution and refinement were performed by using the TEXSAN package of programs. The data were corrected for Lorentz and polarization factors and for absorption.[8] The molybdenum atom was located from the Patterson

Table II. Positional Parameters and B(eq) Values for MoCpCl$_2$(PMe$_3$)$_2$

atom	x	y	z	B(eq), Å^2
Mo	0.18639 (4)	0.03434 (5)	0.21693 (4)	1.92 (3)
Cl(1)	0.3099 (2)	−0.0483 (2)	0.3570 (1)	3.83 (8)
Cl(2)	−0.0105 (1)	0.0433 (2)	0.2210 (2)	4.19 (9)
P(1)	0.1697 (1)	0.2091 (2)	0.3478 (1)	2.88 (8)
P(2)	0.1424 (1)	−0.2035 (2)	0.2110 (1)	2.69 (7)
C(1)	0.1791 (7)	0.1782 (8)	0.0901 (5)	4.2 (4)
C(2)	0.1699 (7)	0.0535 (9)	0.0479 (6)	4.5 (4)
C(3)	0.2710 (8)	−0.013 (1)	0.0698 (7)	5.1 (5)
C(4)	0.3363 (7)	0.075 (1)	0.1229 (6)	4.8 (4)
C(5)	0.2837 (7)	0.1895 (9)	0.1367 (5)	4.5 (4)
C(6)	0.2909 (6)	0.2893 (9)	0.3984 (6)	4.8 (4)
C(7)	0.1103 (7)	0.1503 (8)	0.4628 (6)	4.7 (4)
C(8)	0.0841 (7)	0.3468 (8)	0.3113 (8)	5.7 (5)
C(9)	0.0525 (6)	−0.2571 (9)	0.1049 (7)	5.1 (4)
C(10)	0.0749 (6)	−0.2562 (8)	0.3227 (6)	4.5 (4)
C(11)	0.2526 (7)	−0.3198 (8)	0.2070 (7)	5.0 (4)

Table III. Atomic Coordinates ($\times 10^4$) and Isotropic Thermal Parameters (Å$^2 \times 10^3$) for 3

	x	y	z	U^a
Mo	2987.6 (5)	2500	126.0 (5)	39.4 (2)
I	2354.3 (4)	254.7 (5)	−651.2 (5)	83.3 (2)
P(1)	4026 (2)	2500	−1497 (2)	52.3 (7)
P(2)	1109 (2)	2500	771 (2)	55.7 (7)
C(1)	3194 (8)	2500	1900 (7)	66 (3)
C(2)	3665 (6)	1484 (7)	1501 (5)	69 (2)
C(3)	4494 (5)	1853 (7)	864 (5)	71 (2)
C(4)	3197 (11)	2500	−2602 (9)	79 (4)
C(5)	4939 (6)	3749 (6)	−1711 (6)	72 (2)
C(6)	80 (9)	2500	−211 (9)	95 (5)
C(7)	713 (7)	1210 (10)	1543 (7)	85 (3)

^{a} Equivalent isotropic U defined as one-third of the trace of the orthogonalized U_{ij} tensor.

map, and the rest of the non-hydrogen atoms were found by subsequent alternate least-squares cycles of refinement and difference Fourier maps. At the end of the anisotropic refinement, a difference Fourier map showed all the hydrogen atoms. However, these were introduced in the atom list at calculated positions and used for structure factor calculations but not refined. Their temperature factor was fixed to 1.2 times the equivalent isotropic temperature factor of the corresponding carbon atom. The agreement factor converged to 0.049. An additional absorption correction[9] was applied before the final anisotropic refinement, which converged to $R = 0.041$ ($R_w = 0.057$). Fractional atomic coordinates are in Table II, and selected bond distances and angles are listed in Tables VI and VII.

(8) North, A. C. T.; Phillips, D. C.; Mathews, F. S. *Acta Crystallogr., Sect. A* **1968**, *A24*, 351.

(9) Walker, N.; Stuart, D. *Acta Crystallogr., Sec. A* **1983**, *A39*, 158.
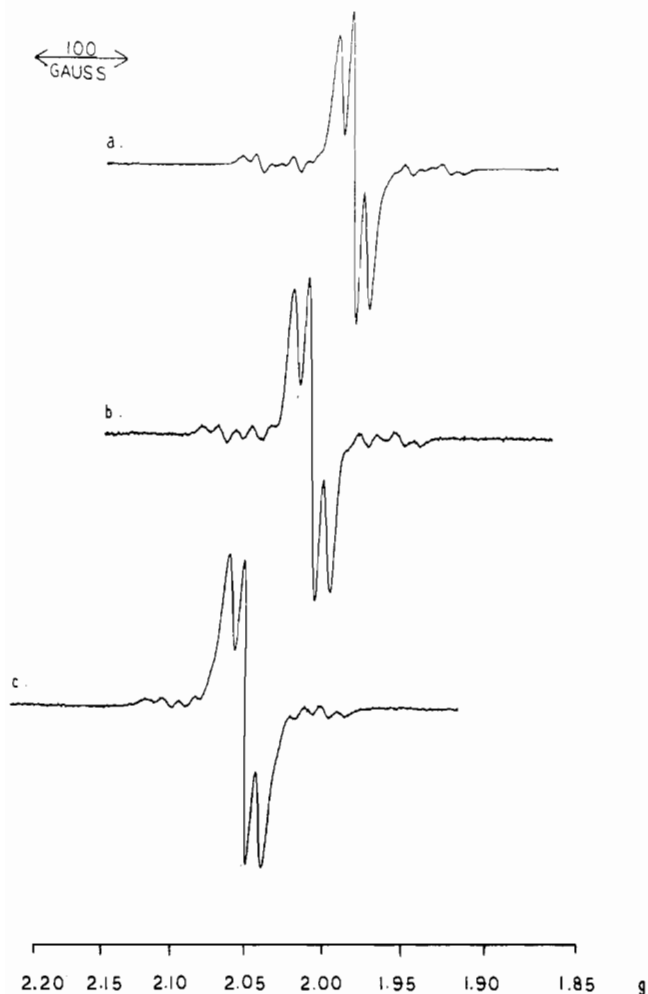
Figure 1. Room-temperature X-band EPR spectra of $MoX_2Cp(PMe_3)_2$ with X = Cl (a), Br (b), and I (c). Solvent = toluene; frequency = 9.47 GHz.

Table IV. Atomic Coordinates ($\times 10^4$) and Temperature Factors ($Å^2 \times 10^3$) for **5**

atom	x	y	z	U^a
Mo	5000	5000	5000	36 (1)
Br	5000	5000	2871 (1)	56 (1)
P	6816 (1)	6816 (1)	4685 (1)	46 (1)
C(1)	7635 (5)	7635 (5)	5863 (6)	72 (2)
C(2)	8331 (4)	6301 (5)	3880 (4)	62 (1)

^{a} Equivalent isotropic U defined as one-third of the trace of the orthogonalized U_{ij} tensor.

(b) $MoCpI_2(PMe_3)_2$ (3). Dark orange crystals of **3** (0.25 × 0.28 × 0.35 mm) were mounted on a glass fiber with epoxy cement. Unit cell parameters were determined by a least-squares fit of 25 reflections (20 ≤ 2θ ≤ 25°). An empirical absorption correction (6 reflections, ψ scan, 216 data) was applied to the collected diffraction data. Crystal data are collected in Table I, final positional parameters are reported in Table III, and selected bond distances and angles are listed in Tables VI and VII. All computer programs are from the SHELXTL (Sheldrick, 1984) and P3 (Nicolet XRD, Madison, WI) program libraries.

The structure was solved by direct methods (SOLV), which located the Mo and I atoms. The remaining non-hydrogen atoms were located through subsequent Fourier syntheses and least-squares refinement. All non-hydrogen atoms were refined anisotropically; H atoms were calculated and fixed in idealized positions (d_{C-H} = 0.960 Å, U = 1.2U of the attached C atom). Systematic absences in the diffraction data suggest two possible space groups—$Pn2_1a$ and $Pnma$—for **3**. $Pnma$ was initially chosen due to the distribution of E values and latter verified by the chemically sensible results of refinement.

(c) $MoBr_2(PMe_3)_4$ (5). Crystal mounting, cell determination, and data collection and reduction were performed as described for $MoCpI_2(PMe_3)_2$ (3). Crystal data are collected in Table I, fractional atomic coordinates are listed in Table IV, and bond distances and angles are in

Table V. Positional Parameters and B(eq) Values for $[MoCpCl_2(PMe_3)_2]^+[PF_6]^{-a}$

atom	x	y	z	B(eq), $Å^2$
Mo	0.3874 (1)	0.01274 (4)	0.24608 (5)	3.00 (3)
Cl(1)	0.5967 (4)	−0.0077 (1)	0.1326 (2)	4.0 (1)
Cl(2)	0.0634 (4)	0.0436 (2)	0.2112 (2)	5.5 (2)
P(1)	0.4216 (4)	0.1304 (1)	0.1865 (2)	3.6 (1)
P(2)	0.2469 (4)	−0.0940 (1)	0.1754 (2)	3.8 (1)
C(1)	0.339 (2)	0.013 (2)	0.3997 (9)	8 (1)
C(2)	0.469 (4)	0.0600 (7)	0.389 (1)	7 (1)
C(3)	0.628 (2)	0.029 (1)	0.3626 (9)	6.5 (9)
C(4)	0.589 (3)	−0.039 (1)	0.3581 (8)	6.8 (9)
C(5)	0.409 (3)	−0.046 (1)	0.383 (1)	7 (1)
C(6)	0.663 (2)	0.1633 (6)	0.1928 (9)	5.4 (7)
C(7)	0.289 (2)	0.1943 (6)	0.2410 (9)	5.7 (7)
C(8)	0.333 (2)	0.1363 (7)	0.0669 (8)	5.9 (7)
C(9)	0.410 (2)	−0.1622 (7)	0.177 (1)	6.6 (8)
C(10)	0.039 (2)	−0.1269 (7)	0.2214 (8)	6.0 (7)
C(11)	0.169 (2)	−0.0812 (6)	0.0563 (8)	5.1 (6)
P(3)	0.9851 (5)	0.3134 (2)	0.9949 (2)	4.8 (2)
F(1)	0.972 (3)	0.383 (1)	1.046 (2)	9.2 (5)
F(2)	1.211 (4)	0.319 (1)	1.007 (2)	11.2 (6)
F(3)	0.965 (3)	0.273 (1)	1.081 (2)	10.3 (5)
F(4)	1.025 (3)	0.249 (1)	0.937 (1)	8.9 (5)
F(5)	0.755 (3)	0.314 (1)	0.967 (2)	11.0 (6)
F(6)	1.001 (3)	0.357 (1)	0.905 (1)	8.1 (4)
F(1′)	1.132 (3)	0.315 (1)	1.085 (1)	9.4 (5)
F(2′)	0.807 (3)	0.322 (1)	1.054 (2)	10.0 (5)
F(3′)	0.953 (3)	0.237 (1)	1.007 (2)	11.9 (7)
F(4′)	0.844 (4)	0.308 (1)	0.906 (2)	13.0 (7)
F(5′)	1.159 (5)	0.307 (2)	0.942 (2)	16 (1)
F(6′)	0.978 (5)	0.389 (2)	0.988 (2)	17 (1)

^{a} Numbers in parentheses are standard deviations in the least significant digit.

Table VI. Selected Intramolecular Distances (Å) for $MoCpX_2(PMe_3)_2$ (X = Cl, I) and $MoCpCl_2(PMe_3)_2]PF_6{}^a$

$MoCpCl_2(PMe_3)_2$ (1)		$[MoCpCl_2(PMe_3)_2]$- PF_6 (6)		$MoCpI_2(PMe_3)_2$ (3)	
Mo–Cl(1)	2.468 (2)	Mo–Cl(1)	2.374 (3)	Mo–I	2.831 (1)
Mo–Cl(2)	2.474 (2)	Mo–Cl(2)	2.369 (3)		
Mo–P(1)	2.484 (2)	Mo–P(1)	2.531 (3)	Mo–P(1)	2.500 (2)
Mo–P(2)	2.481 (2)	Mo–P(2)	2.530 (3)	Mo–P(2)	2.502 (2)
Mo–C(1)	2.208 (7)	Mo–C(1)	2.32 (1)	Mo–C(1)	2.349 (9)
Mo–C(2)	2.214 (7)	Mo–C(2)	2.32 (1)	Mo–C(2)	2.300 (7)
Mo–C(3)	2.305 (8)	Mo–C(3)	2.31 (1)	Mo–C(3)	2.243 (7)
Mo–C(4)	2.346 (8)	Mo–C(4)	2.31 (1)		
Mo–C(5)	2.289 (7)	Mo–C(5)	2.32 (1)		
P(1)–C(6)	1.811 (8)	P(1)–C(6)	1.82 (1)	P(1)–C(4)	1.788 (12)
P(1)–C(7)	1.821 (7)	P(1)–C(7)	1.82 (1)	P(1)–C(5)	1.830 (7)
P(1)–C(8)	1.810 (8)	P(1)–C(8)	1.81 (1)		
P(2)–C(9)	1.814 (8)	P(2)–C(9)	1.78 (1)	P(2)–C(6)	1.826 (12)
P(2)–C(10)	1.814 (8)	P(2)–C(10)	1.80 (1)	P(2)–C(7)	1.835 (10)
P(2)–C(11)	1.822 (8)	P(2)–C(11)	1.80 (1)		
C(1)–C(2)	1.38 (1)	C(1)–C(2)	1.34 (2)	C(1)–C(2)	1.386 (9)
C(1)–C(5)	1.41 (1)	C(1)–C(5)	1.31 (2)	C(2)–C(3)	1.397 (10)
C(2)–C(3)	1.45 (1)	C(2)–C(3)	1.37 (2)	C(3)–C(3′)	1.452 (16)
C(3)–C(4)	1.37 (1)	C(3)–C(4)	1.39 (2)		
C(4)–C(5)	1.36 (1)	C(4)–C(5)	1.35 (2)		

^{a} Estimated standard deviations in the least significant figure are given in parentheses.

Table VIII. The structure of **5** is isomorphous with that of the Cl analogue;[10] refinement was initiated with the heavy-atom coordinates from the Cl analogue. All non-hydrogen atoms were refined anisotropically; all H atoms were found and refined isotropically.

(d) $[MoCpCl_2(PMe_3)_2]PF_6$ (6). Crystal mounting, cell determination, data collection and reduction, and the structure solution and refinement were carried out as described above for $MoCpCl_2(PMe_3)_2$. Crystal data are in Table I. The PF_6^- anion was found to be disordered among two equally populated positions. The fluorine atoms were refined isotropically. The hydrogen atoms were included at calculated positions and used for structure factor calculations but not refined. Their temperature factor was fixed to 1.2 times the equivalent isotropic temperature factor of the

(10) Carmona, E.; Marin, J. M.; Poveda, M. L.; Atwood, J. L.; Rogers, R. D. *Polyhedron* **1983**, *2*, 185.

Table VII. Selected Intramolecular Angles (deg) for $MoCpX_2(PMe_3)_2$ (X = Cl, I) and $MoCpCl_2(PMe_3)_2]PF_6{}^a$

$MoCpCl_2(PMe_3)_2$ (1)		$[MoCpCl_2(PMe_3)_2]PF_6$ (6)		$MoCpI_2(PMe_3)_2$ (3)	
Cl(1)–Mo–Cl(2)	125.14 (7)	Cl(1)–Mo–Cl(2)	123.0 (1)	I–Mo–I′	125.6 (1)
Cl(1)–Mo–P(1)	79.01 (6)	Cl(1)–Mo–P(1)	80.1 (1)	I–Mo–P(1)	80.6 (1)
Cl(1)–Mo–P(2)	79.56 (6)	Cl(1)–Mo–P(2)	79.0 (1)	I–Mo–P(2)	81.9 (1)
Cl(1)–Mo–C(1)	140.9 (2)	Cl(1)–Mo–C(1)	148.2 (4)	I–Mo–C(1)	112.9 (1)
Cl(1)–Mo–C(2)	141.6 (2)	Cl(1)–Mo–C(2)	126.4 (8)	I–Mo–C(2)	87.0 (2)
Cl(1)–Mo–C(3)	104.3 (3)	Cl(1)–Mo–C(3)	95.0 (5)	I–Mo–C(3)	96.0 (2)
Cl(1)–Mo–C(4)	87.9 (2)	Cl(1)–Mo–C(4)	92.7 (4)	I–Mo–C(2′)	145.9 (2)
Cl(1)–Mo–C(5)	104.3 (2)	Cl(1)–Mo–C(5)	122.0 (7)	I–Mo–C(3′)	132.8 (2)
Cl(2)–Mo–P(1)	80.25 (6)	Cl(2)–Mo–P(1)	78.8 (1)		
Cl(2)–Mo–P(2)	79.41 (6)	Cl(2)–Mo–P(2)	78.6 (1)		
Cl(2)–Mo–C(1)	89.9 (2)	Cl(2)–Mo–C(1)	88.7 (4)		
Cl(2)–Mo–C(2)	89.4 (2)	Cl(2)–Mo–C(2)	103.6 (7)		
Cl(2)–Mo–C(3)	122.6 (3)	Cl(2)–Mo–C(3)	137.9 (6)		
Cl(2)–Mo–C(4)	147.0 (2)	Cl(2)–Mo–C(4)	141.2 (6)		
Cl(2)–Mo–C(5)	123.1 (3)	Cl(2)–Mo–C(5)	107.3 (6)		
P(1)–Mo–P(2)	133.66 (6)	P(1)–Mo–P(2)	133.5 (1)	P(1)–Mo–P(2)	141.2 (1)
P(1)–Mo–C(1)	92.4 (2)	P(1)–Mo–C(1)	111.6 (8)	P(1)–Mo–C(1)	142.3 (2)
P(1)–Mo–C(2)	128.1 (2)	P(1)–Mo–C(2)	85.0 (4)	P(1)–Mo–C(2)	118.7 (2)
P(1)–Mo–C(3)	141.9 (2)	P(1)–Mo–C(3)	92.2 (5)	P(1)–Mo–C(3)	86.1 (2)
P(1)–Mo–C(4)	110.0 (3)	P(1)–Mo–C(4)	126.3 (7)		
P(1)–Mo–C(5)	83.9 (2)	P(1)–Mo–C(5)	140.6 (4)		
P(2)–Mo–C(1)	128.6 (2)	P(2)–Mo–C(1)	108.0 (8)	P(2)–Mo–C(1)	76.5 (2)
P(2)–Mo–C(2)	92.8 (2)	P(2)–Mo–C(2)	139.9 (5)	P(2)–Mo–C(2)	94.6 (2)
P(2)–Mo–C(3)	83.3 (2)	P(2)–Mo–C(3)	130.6 (6)	P(2)–Mo–C(3)	130.1 (2)
P(2)–Mo–C(4)	109.7 (3)	P(2)–Mo–C(4)	95.9 (6)		
P(2)–Mo–C(5)	141.4 (2)	P(2)–Mo–C(5)	85.2 (4)		
C(1)–Mo–C(2)	36.5 (3)	C(1)–Mo–C(2)	33.5 (6)	C(1)–Mo–C(2)	34.7 (2)
C(1)–Mo–C(3)	60.7 (3)	C(1)–Mo–C(3)	56.3 (5)	C(1)–Mo–C(3)	58.5 (3)
C(1)–Mo–C(4)	59.1 (3)	C(1)–Mo–C(4)	56.2 (5)		
C(1)–Mo–C(5)	36.6 (3)	C(1)–Mo–C(5)	32.8 (6)		
C(2)–Mo–C(3)	37.3 (3)	C(2)–Mo–C(3)	34.4 (5)	C(2)–Mo–C(3)	35.8 (2)
C(2)–Mo–C(4)	59.2 (3)	C(2)–Mo–C(4)	57.1 (5)	C(2)–Mo–C(3′)	60.6 (3)
C(2)–Mo–C(5)	60.0 (3)	C(2)–Mo–C(5)	55.6 (5)	C(2)–Mo–C(2′)	59.4 (4)
C(3)–Mo–C(4)	34.2 (3)	C(3)–Mo–C(4)	34.9 (6)	C(3)–Mo–C(3′)	37.8 (4)
C(3)–Mo–C(5)	58.3 (3)	C(3)–Mo–C(5)	56.5 (5)		
C(4)–Mo–C(5)	34.1 (3)	C(4)–Mo–C(5)	34.0 (5)		
Mo–P(1)–C(6)	117.9 (3)	Mo–P(1)–C(6)	116.1 (4)	Mo–P(1)–C(4)	113.1 (4)
Mo–P(1)–C(7)	113.0 (3)	Mo–P(1)–C(7)	115.4 (4)	Mo–P(1)–C(5)	117.2 (2)
Mo–P(1)–C(8)	116.6 (3)	Mo–P(1)–C(8)	111.3 (5)		
C(6)–P(1)–C(7)	103.0 (4)	C(6)–P(1)–C(7)	104.2 (6)	C(4)–P(1)–C(5)	103.7 (4)
C(6)–P(1)–C(8)	102.5 (4)	C(6)–P(1)–P(8)	104.6 (6)	C(5)–P(1)–C(5′)	99.9 (5)
C(7)–P(1)–C(8)	101.8 (4)	C(7)–P(1)–C(8)	104.0 (6)		
Mo–P(2)–C(9)	116.3 (3)	Mo–P(2)–C(9)	114.5 (5)	Mo–P(2)–C(6)	115.1 (4)
Mo–P(2)–C(10)	112.2 (3)	Mo–P(2)–C(10)	116.8 (4)	Mo–P(2)–C(7)	116.2 (3)
Mo–P(2)–C(11)	117.8 (3)	Mo–P(2)–C(11)	110.3 (4)		
C(9)–P(2)–C(10)	103.2 (4)	C(9)–P(2)–C(10)	105.4 (7)	C(6)–P(2)–C(7)	101.6 (4)
C(9)–P(2)–C(11)	102.6 (4)	C(9)–P(2)–C(11)	104.7 (6)	C(7)–P(2)–C(7′)	104.0 (3)
C(10)–P(2)–C(11)	103.0 (4)	C(10)–P(2)–C(11)	103.9 (6)		
C(2)–C(1)–C(5)	107.3 (8)	C(2)–C(1)–C(5)	109 (2)	C(2)–C(1)–C(2′)	110.5 (9)
C(1)–C(2)–C(3)	107.4 (7)	C(1)–C(2)–C(3)	108 (2)	C(1)–C(2)–C(3)	107.5 (7)
C(2)–C(3)–C(4)	106.5 (8)	C(2)–C(3)–C(4)	107 (1)	C(2)–C(3)–C(3′)	107.2 (5)
C(3)–C(4)–C(5)	110.3 (8)	C(3)–C(4)–C(5)	106 (1)		
C(1)–C(5)–C(4)	108.5 (7)	C(1)–C(5)–C(4)	110 (2)		

^{a} Estimated standard deviations in the least significant figure are given in parentheses.

corresponding carbon atom. Fractional atomic coordinates are listed in Table V, and selected bond distances and angles are compared with those of compounds 1 and 3 in Tables VI and VII.

Theoretical Calculations. The Fenske–Hall[11] molecular orbital treatment was employed on the model compounds $MoCpX_2(PH_3)_2$ (X = Cl, I). The atomic 1s, 2s, 2p, 3s, 3p, 3d, 4s, and 4p orbitals of the Mo and I atoms and the 1s, 2s, and 2p orbitals of the Cl and P atoms were treated as a "core". The phosphorus 3d orbitals were included in the calculations, whereas for all the other atoms a minimum basis set was employed. Atomic parameters from the $MoCpCl_2(PMe_3)_2$ and Mo-$CpI_2(PMe_3)_2$ crystal structures idealized to C_s symmetry were employed. All chemically equivalent bond distances and angles were averaged, and the hydrogen atoms of the PH_3 ligands were placed along the directions where the CH_3 carbon atoms were found in the crystal structures, with a P–H bond length of 1.44 Å. The Cp hydrogen atoms (not seen in the crystal structures) were placed at calculated positions at a distance of 1.09 Å from the corresponding carbon atom. A right-handed coordinate system was chosen, with the z axis pointing from the molybdenum atom

(11) Hall, M. B.; Fenske, R. F. *Inorg. Chem.* **1972,** *11*, 768.

Table VIII. Intramolecular Bond Distances (Å) and Angles (deg) for $MoBr_2(PMe_3)_4$ (5)

Distances			
Mo–Br	2.614 (1)	P–C(1)	1.829 (7)
Mo–P	2.514 (1)	P–C(2)	1.836 (4)
Angles			
Br–Mo–Br(a)	180	P–Mo–P(b)	162.3 (1)
Br–Mo–P	81.2 (1)	Mo–P–C(1)	118.9 (2)
Br–Mo–P(a)	98.8 (1)	Mo–P–C(2)	116.8 (1)
P–Mo–P(a)	91.4 (1)		

toward the center of the Cp ring. The local coordinate systems on the chlorine and phosphorus atoms were chosen such that the z axis on each atom points toward the molybdenum atom.

Results

(a) Syntheses. The compounds $MoX_3(PMe_3)_3$ (X = Cl, Br, I) reacted with TlCp in either THF or toluene to afford the slightly air-sensitive products $MoCpX_2(PMe_3)_2$ [X = Cl (1), Br (2), I (3)] in moderate yields (eq 1).

$$MoX_3(PMe_3)_3 + TlCp \rightarrow MoCpX_2(PMe_3)_2 + TlX + PMe_3 \tag{1}$$

This reaction also afforded variable amounts of other products, depending on reaction conditions. These have been identified as $Mo_2X_4(PMe_3)_4$ and $MoX_2(PMe_3)_4$. Small amounts of unreacted starting material were also found in the final reaction mixtures (UV/visible monitoring). Reaction 1 slowly takes place at room temperature, as evidenced by EPR monitoring of the product formation, but it is not possible to take it to completion under these conditions. Subsequent warming helps the reaction to proceed to a further extent but also causes the formation of the molybdenum(II) byproducts. We believe this effect to be due to the precipitation of the thallium halide on top of the unreacted cyclopentadienylthallium, slowing down the interaction between the two reactants and eventually stopping the reaction before all the Cp reagent has been consumed. We found no interaction to occur with NaCp.

The conditions reported in the Experimental Section for the synthesis of these materials are those found to maximize the product formation and minimize the decomposition to the Mo(II) byproducts. The reactions on the bromide and chloride systems (especially the latter) give the best results in THF. The use of toluene as solvent gives extensive decomposition in these cases. For the iodide reaction, on the other hand, although the product indeed forms in THF, this happens at a slower rate. Toluene gives the best result in this case with only a minor amount of decomposition products. These observations suggest a reaction rate for equation 1 in the order Cl > Br > I and a decomposition rate following the same order.

Reaction 1 releases 1 mol of PMe_3/mol of product. Since the Mo(III) starting material is obtained from $MoX_3(THF)_3$ and PMe_3, we tested the syntheses of compounds 1–3 directly from $MoX_3(THF)_3$, TlCp, and 2 equiv of PMe_3. Although we did observe (by EPR spectroscopy) the formation of the products in both toluene and THF, this procedure was in general inferior to that illustrated in eq 1.

The $Mo_2X_4(PMe_3)_4$ byproducts were identified qualitatively by visible spectroscopy and not isolated. These compounds are all known in the literature (X = Cl,[12] Br,[13] I[13b,14]). They display a very characteristic visible absorption band, assigned to a $\delta \rightarrow \delta^*$ transition, whose frequency is sensitive to the nature of the halide.[15] The $MoX_2(PMe_3)_4$ byproducts were isolated for X = Cl (4) and Br (5) and characterized by elemental analysis and optical spectroscopy and for X = Br by X-ray crystallography. Compound 4 had already been described.[10]

Since we obtained electrochemical evidence (vide infra) of a reversible one-electron oxidation of compounds 1–3 to the corresponding Mo(IV) cations, we have accomplished the chemical oxidation of the chloride species according to eq 2.

$$MoCpCl_2(PMe_3)_2 + AgPF_6 \rightarrow [MoCpCl_2(PMe_3)_2]PF_6 + Ag \tag{2}$$
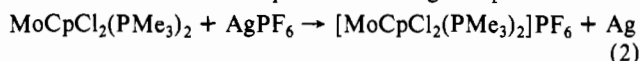
The reaction proceeds instantaneously in CH_2Cl_2 at room temperature. The air-stable product $[MoCpCl_2(PMe_3)_2]PF_6$ (6) was crystallized by diffusion of ether into a CH_2Cl_2 solution and characterized by a variety of techniques, including X-ray crystallography. This compound is similar to other monocyclopentadienylmolybdenum(IV) derivatives reported by Green and co-workers,[16] e.g. $MoCpCl_3(L_2)$ (L_2 = chelating diphosphine), with the notable difference of the electron count (vide infra).

Table IX. EPR Spectral Parameters for Mo(III)–Cp Derivatives

compd	g	a_{Mo}: 10^{-3} cm^{-1} (G)	a_P: 10^{-3} cm^{-1} (G)	ref
MoCpCl₂(PMe₃)₂ (1)	1.982	3.79 (41.0)	1.39 (15.0)	this work
MoCpBr₂(PMe₃)₂ (2)	2.006	3.70 (39.5)	1.64 (17.5)	this work
MoCpI₂(PMe₃)₂ (3)	2.046	3.34 (35.0)	1.72 (18.0)	this work
MoCp*Cl₂(PMe₃)₂[a]	1.984	3.24 (35.0)	1.38 (14.9)	4c
MoCp'Cl₂(PMe₃)₂[b]	1.983	3.43 (37)	NR[c]	4b
MoCp'Cl₂(PMe₂Ph)₂[b]	1.988	3.90 (42)	1.02 (11)	4b

[a] $Cp^* = \eta^5\text{-}C_5Me_5$. [b] $Cp' = \eta^5\text{-}(i\text{-Pr})C_5H_4$. [c] NR = not reported.

(b) Spectroscopic Characterization. **(i) $MoCpX_2(PMe_3)_2$.** Compounds 1–3 exhibit effective magnetic moments consistent with one unpaired electron both in the solid state and in solution (Evans method).[17] These were 1.72 (1), 1.68 (2), and 1.61 μ_B (3). Both EPR spectroscopy and MO calculations by the Fenske–Hall method (vide infra) suggest that the compounds are in a pure low-spin configuration. Magnetic studies for low-spin Mo(III) compounds are few, mainly because most Mo(III) compounds have a pseudooctahedral geometry and a high-spin ($S = {}^3/_2$) electronic ground state.[18] The compound $K_4Mo(CN)_7\cdot 2H_2O$ has an effective magnetic moment of 1.73 μ_B, independent of temperature.[19] No magnetic data were reported for compounds $Mo(\eta^5\text{-}C_5H_4R)Cl_2L_2$ [R = i-Pr; L = PMe_3, PMe_2Ph; L_2 = bis-(diisopropylphosphino)ethane].[4]

The room-temperature EPR spectra of compounds 1–3 are shown in Figure 1. They exhibit a more intense 1:2:1 triplet due to the coupling to two equivalent phosphorus nuclei in the fraction of molecules containing inactive molybdenum nuclei ($I = 0$, total natural abundance ca. 75%), consistent with the presence of two phosphine ligands in equivalent positions. The other, less intense absorptions can be described as a sextet of triplets generated by the rest of the species (⁹⁵Mo and ⁹⁷Mo, $I = {}^5/_2$, similar nuclear magnetic moments; total abundance ca. 25%). We do not observe splitting due to the halogen nuclei.

The literature is very limited on EPR spectroscopic studies of Mo(III) compounds. Mononuclear complexes are typically six-coordinated in the $S = {}^3/_2$ spin state. In general, extremely broad signals can be observed at temperatures lower than those attainable with liquid nitrogen.[20] One Mo(III) species in the $S = {}^1/_2$ state that has been investigated by EPR techniques is $[Mo(CN)_7]^{4-}$.[19] Even this compound, however, shows a very broad signal with no indication of hyperfine splitting at temperatures below 150 K.[19] The mononuclear molybdenum(III) cyclopentadienyl derivatives described in the literature[4] display EPR spectra analogous to those of compounds 1–3. Other compounds exhibiting relatively sharp EPR spectra are the mixed-valence $(CpMo)_2(\mu\text{-S})(\mu\text{-SCH}_3)S_2CH_2$[2g] and $(CpMo)_2(S_2CH_2)(\mu\text{-S})(\mu\text{-SCH}=CPhH)$[2j] also containing Cp rings.

The g factors and the hyperfine splitting a_{Mo} and a_P parameters of compounds 1–3 are reported in Table IX and compared with those of other known molybdenum(III) cyclopentadienyl compounds. The g values are close to the free spin value. The molybdenum hyperfine splitting constants are all around 40 G, and the phosphorus hyperfine splitting constants are in the range 10–20 G, being smaller for X = Cl and larger for X = I.

The optical spectra of compounds 1–3 show activity only in the UV region, no absorption bands being observed in the visible and near-IR portions up to 900 nm. The IR spectra exhibit the typical absorption bands of the cyclopentadienyl and trimethylphosphine moieties.

(ii) $[MoCpCl_2(PMe_3)_2]PF_6$. Compound 6 is, unexpectedly, paramagnetic. Its solid-state room-temperature magnetic moment of 2.42 μ_B is well within the range found for other d² Mo(IV)

(12) Cotton, F. A.; Extine, M. W.; Felthouse, T. R.; Kolthammer, B. W.; Lay, D. G. *J. Am. Chem. Soc.* **1981**, *103*, 4040.
(13) (a) Brown, P. R.; Cloke, F. G. N.; Green, M. L. H.; Tovey, R. C. *J. Chem. Soc., Chem. Commun.* **1982**, 519. (b) Hopkins, M. D.; Schaefer, W. P.; Bronikowski, M. J.; Woodruff, W. H.; Miskowski, V. M.; Dallinger, R. F.; Gray, H. B. *J. Am. Chem. Soc.* **1987**, *109*, 408.
(14) (a) Cotton, F. A.; Poli, R. *J. Am. Chem. Soc.* **1986**, *108*, 5628. (b) Cotton, F. A.; Poli, R. *Inorg. Chem.* **1987**, *26*, 3228.
(15) Hopkins, M. D.; Gray, H. B.; Miskowski, V. M. *Polyhedron* **1987**, *6*, 705.
(16) (a) Aviles, T.; Green, M. L. H.; Dias, A. R.; Romao, C. *J. Chem. Soc., Dalton Trans.* **1979**, 1367. (b) Adams, G. S. B.; Green, M. L. H. *J. Chem. Soc., Dalton Trans.* **1981**, 353.

(17) Evans, D. F.; James, T. A. *J. Chem. Soc., Dalton Trans.* **1979**, 723.
(18) Figgis, B. N.; Lewis, J. *Prog. Inorg. Chem.* **1964**, *6*, 37.
(19) Rossman, G. R.; Tsay, F.-D.; Gray, H. B. *Inorg. Chem.* **1973**, *12*, 824.
(20) (a) Jarrett, H. S. *J. Chem. Phys.* **1957**, *27*, 1298. (b) Mitchell, P. C. H.; Scarle, R. D. *J. Chem. Soc., Dalton Trans.* **1975**, 110. (c) Averill, B. A.; Orme-Johnson, W. H. *Inorg. Chem.* **1980**, *19*, 1702. (d) Millar, M.; Lincoln, S.; Koch, S. A. *J. Am. Chem. Soc.* **1982**, *104*, 288.

complexes, the decrease with respect to the spin-only value being attributed to large spin–orbit-coupling effects.[18] The NMR spectroscopic properties could not be observed because of the paramagnetism and sparing solubility of the compound.
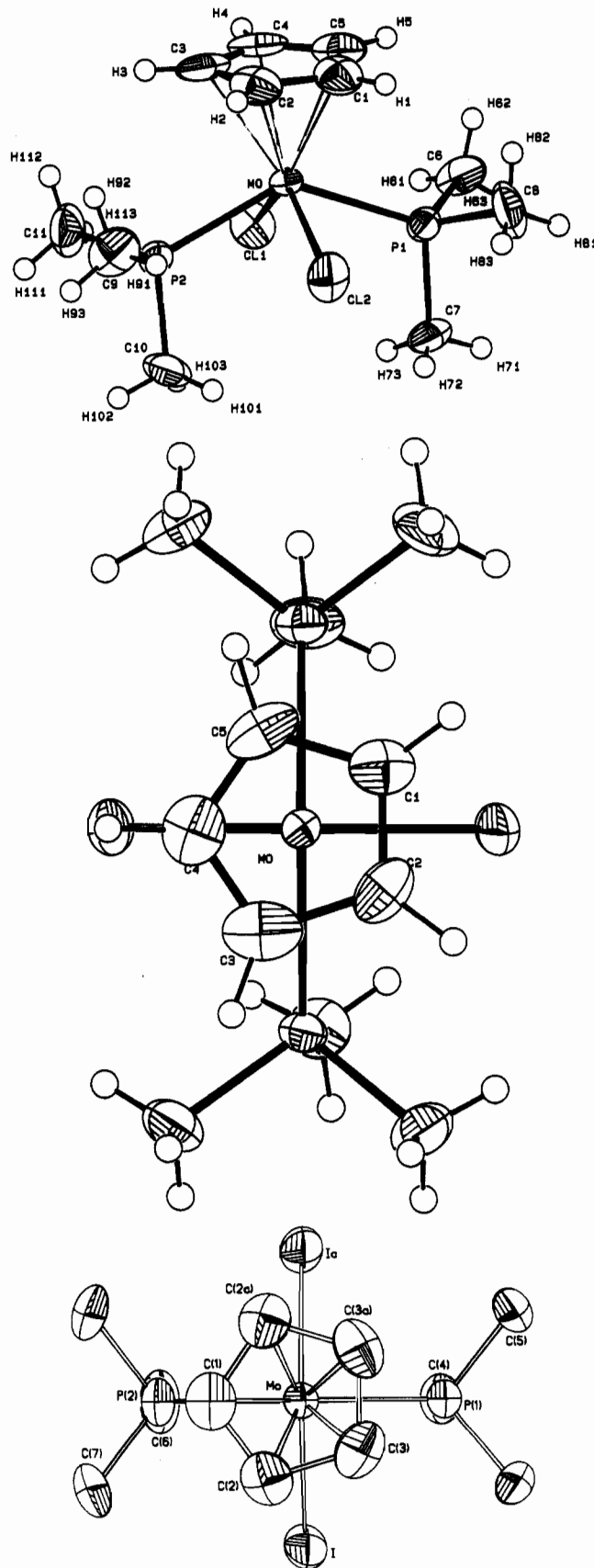
The IR spectrum shows the same absorptions seen for compound **1**, plus a strong band (with shoulders) at 835 cm⁻¹ and a medium one at 555 cm⁻¹. These can be attributed to the two IR-active T_{1u} stretching and bending vibrations, respectively, of the octahedral PF_6^- ion, the former possibly being split by a reduction of symmetry in the crystalline environment. Their values are very close to those calculated for the octahedral ion (850 and 555 cm⁻¹),[21] suggesting that the cation and anion do not engage in interactions other than the electrostatic attraction.

The UV/visible spectrum shows a strong absorption in the UV region, plus two bands of approximately the same intensity at 323 and 474 nm.

(c) Crystal Structures. (i) $MoCpX_2(PMe_3)_2$ (X = Cl, I). On the basis of the EPR data reported above, a mononuclear, four-legged piano-stool configuration seems likely for compounds **1–3**. Both a trans and a cis relative arrangement of the phosphine ligands are in accord with the EPR observation of two equivalent phosphorus nuclei. The X-ray structural determination on compounds **1** and **3** shows (Figure 2) that the trans arrangement is the preferred one, as might have been expected on steric grounds. The chloride compound crystallizes in the monoclinic space group $P2_1/a$ with the entire molecule in the asymmetric unit. The molecule, however, has ideal C_s symmetry, the mirror plane passing through atoms Mo, C(4), H(4), Cl(1), and Cl(2) (see Figure 2b). On the other hand, the iodide compound crystallizes in the orthorhombic space group *Pnma* and the molecule has a crystallographically imposed mirror plane, which passes through atoms Mo, C(1), H(1), P(1), P(2), C(4), and C(6) (see Figure 2c). It is interesting to note that in **1** the Cp unique carbon is eclipsed with a chloro ligand, whereas in **3** this is eclipsed with a phosphine ligand. This probably means that the relative orientation of the Cp ring for each compound is not determined by electronic effects but merely by packing forces.

The Mo–C(Cp) distances (average: **1**, 2.272 Å; **3**, 2.287 Å) are slightly shorter than those found in other Mo(III)–Cp structures (in the range 2.301–2.324 Å).[2f,3] It is to be noted that the Mo–C distances vary over a wide range (2.21–2.35 Å for **1**, 2.24–2.35 Å for **3**). An examination of the C–C bond distances also reveals a spread, consistent with the Cp ligand having some η^3,η^2 character. The carbons of the η^3 system (C(3), C(4), and C(5) for **1**; C(1), C(2), and C(2') for **3**) are farther away from the metal than those of the η^2 system. The opposite trend is observed for compounds $Re(\eta^5\text{-}C_5Me_5)X_2O$ (X = Cl, I, CH₃).[22a] In the latter example a strong trans influence of the oxo ligand is believed to be responsible for the Cp ring rearrangement. Hoffmann et al.[22b] have attributed distorsions of the type observed by us to the presence of a significant metal–Cp δ interaction.

The Mo–Cl distance in compound **1** [average 2.471 (3) Å] and the Mo–I distance in compound **3** (2.831 Å) are longer than normal {e.g. (averaged figures are listed): for Mo(III)–Cl, 2.428 (8) Å in $MoCl_3(py)_3$,[23a] 2.452 (13) Å in $[Ph_2HP-(CH_2)_2PHPh_2]_3[MoCl_6]_2\cdot12H_2O$,[23b] 2.433 (4) Å in $[PPh_4]_2-[Mo_2(O_2CPh)_4Cl_4]$,[24] and 2.436 (7) Å in $Mo_4Cl_4(O\text{-}i\text{-}Pr)_8$;[25] for Mo(III)–I, 2.763 (9) and 2.77 (2) Å in two different salts of the $[Mo_2I_7(PMe_3)_2]^-$ ion,[26] 2.77 (2) Å in *mer*-MoI₃(THF)₃,[6] 2.760 (8) Å in MoI₃(dppe)(THF),[7] 2.768 (7) Å in MoI₃(dppe)(PMe₃),[7] and 2.77 (3) Å in *mer*-MoI₃(PMe₃)₃[7]}. The Mo–P distances [average 2.482 (2) Å], on the other hand, are shorter than those

(21) Mayfield, H. G.; Bull, W. E. *J. Chem. Soc.* **1971**, 2280.
(22) (a) Herrmann, W. A.; Herdtweck, E.; Flöel, M.; Kulpe, J.; Küsthardt, U.; Okuda, J. *Polyhedron* **1987**, *6*, 1165. (b) Kubacek, P.; Hoffmann, R.; Havlas, Z. *Organometallics* **1982**, *1*, 180.
(23) (a) Brencic, J. V. *Z. Anorg. Allg. Chem.* **1974**, *403*, 218. (b) Herbowski, A.; Lis, T. *Polyhedron* **1985**, *5*, 127.
(24) Jansen, K.; Dehnicke, K.; Fenske, D. *Z. Naturforsch.* **1987**, *42B*, 1097.
(25) Chisholm, M. H.; Clark, D. L.; Errington, R. J.; Folting, K.; Huffman, J. C. *Inorg. Chem.* **1988**, *27*, 2071.
(26) Cotton, F. A.; Poli, R. *Inorg. Chem.* **1987**, *26*, 3310.

Figure 2. (a, Top) ORTEP view of the $MoCpCl_2(PMe_3)_2$ molecule, showing the numbering scheme employed. Hydrogen atoms are drawn with arbitrary radii. (b, Middle) Top view of the $[MoCpCl_2(PMe_3)_2]^n$ ($n = 0, +1$) species. The numbering scheme shown is that of the Mo(III) neutral molecule. The numbering scheme of the Mo(IV) cation is related to that of the Mo(III) molecule (in parentheses) as follows: Cl1 (Cl2); Cl2 (Cl1); C1 (C4); C2 (C5); C3 (C1); C4 (C2); C5 (C3); C6 (C8); C7 (C6); C8 (C7); C10 (C11); C11 (C10). (c, Bottom) Top view of the $MoCpI_2(PMe_3)_2$ molecule.

found in other PMe₃ compounds of Mo(III) [e.g. 2.554 (15) and 2.546 (3) Å in the above-mentioned salts of $Mo_2I_7(PMe_3)_2^{-26}$ and 2.59 (5) Å in *mer*-$MoI_3(PMe_3)_3$[7]]. This would seem to indicate a softening of the Mo(III) center in these compounds, with stronger interactions to the softer Cp⁻ and PMe₃ ligands and weaker interactions to Cl⁻ and I⁻. It will be shown below that there is indication of Mo–P π back-bonding in these systems. It is conceivable that the presence of a good electron donor such as the Cp ligand raises the energy of the molybdenum atomic orbitals and makes the π-back-bonding mechanism to the phosphine ligands more efficient than in other Mo(III) derivatives. 1 and 3 are the first Mo(III)–Cp–PR₃ derivatives to be characterized by crystallographic methods.

(ii) *trans*-MoBr₂(PMe₃)₄. Compound 5 crystallizes in the tetragonal space group *I*42*m*, with the molecule having crystallographic 42*m* (D_{2d}) symmetry. The structure is isomorphous to that reported for *trans*-MoCl₂(PMe₃)₄.[10] Other Mo(II) crystallographically characterized compounds of similar geometry are *trans*-MoX₂(dppe)₂ (X = Cl,[27] Br[28]), *trans*-MoCl₂(PMe₂Ph)₄,[29] and *trans*-MoCl₂(dmpe)₂.[30] The cis isomer of MoCl₂(dppe)₂ has also been reported.[31]

The structure of compound 5 can be described as a distorted octahedron, with one pair of trans phosphorus atoms lying above, and the other below, the equatorial plane. The P–Mo–P(trans) angle is 162.3 (1)° and compares well with the same angle in the corresponding chloride structure [162.1 (1)°].[10] The Mo–Br distance [2.614 (1) Å] is longer than the same distance found in *trans*-MoBr₂(dppe)₂ [2.569 (1) Å] and in quadruply bonded Mo(II) dimers [e.g. 2.51 (3) Å (average) in Mo₂Br₄-(Ph₂AsCH₂CH₂AsPh₂)₂[32] and 2.547 (1) Å in Mo₂Br₄(PMe₃)₄[13b]]. The Mo–P distance [2.514 (1) Å] is in the same range (2.46–2.55 Å) found for the molybdenum(II)–phosphine derivatives mentioned above.[27–30]

(iii) [MoCpCl₂(PMe₃)₂]PF₆. 6 crystallizes in the monoclinic *P*2₁/*c* space group, with the entire molecule in the asymmetric unit. The cation and anion are well separated from each other. The anion is disordered among two equally populated orientations that have the phosphorus atom in common, one of the 4-fold axes of the first being approximately colinear with one of the 3-fold axes of the second. Each of these orientations has a slightly distorted octahedral geometry, with P–F distances averaging 1.58 (2) and 1.56 (2) Å.

The cation has the same structure as the parent compound 1, including the relative orientation of the Cp ring (see Figure 2b). Bond distances and angles of the two species are compared in Tables VI and VII, together with those of compound 3. The overall geometries of compound 1 and the cation of compound 6 are strikingly similar, all of the bond angles being the same to within a few degrees. The major changes concern the cyclopentadienyl ring, which is, contrary to that in compound 1, fairly regularly placed in a η⁵ piano-stool structure (all Mo–C distances are in the narrow 2.31–2.32 range).

The bond lengths show interesting trends. The Mo–Cl distances (average 2.372 Å) are about 0.1 Å shorter than the same ones found in the parent Mo(III) molecule. This bond shortening is expected and can be attributed to the contraction of the Mo radius upon increase of the oxidation state from +III to +IV. On the other hand, the Mo–P distances in 6 (average 2.530 Å) are about 0.05 Å *longer* than the corresponding distances in 1. This variation is opposite from the expected one and is, we believe, the result of the decrease in Mo to P π-back-donation efficiency on going from compound 1 to compound 6. We may observe that π

back-donation to phosphine ligands has been earlier the subject of some controversy[33] but is now a widely accepted occurrence in low oxidation state complexes.[34] However, evidence of its presence in oxidation states as high as +III is not common. To the best of our knowledge, our example represents the first direct evidence of a M(III) to P π back-donation for any transition-state metal.

The observed Mo–P distances in 6 are in the range found for other Mo(IV)–PR₃ phosphine derivatives, such as [MoOCl-(dppe)₂]⁺ (2.57 Å)[35] and *cis-mer*-MoOCl₂(PR₂Ph)₃ (R = Me,[36a] 2.500–2.558 Å; R = Et,[36b] 2.522–2.580 Å).

The Mo–C(Cp) distances are, like the Mo–P bond lengths, *longer* in the more oxidized material (2.32 vs 2.27 Å). A possible interpretation of this result will be presented in the Discussion, after the examination of the molecular orbital results.

(d) Electrochemical Studies. Compounds 1–3 have been studied electrochemically by cyclic voltammetry in CH₂Cl₂ solutions by using a platinum working electrode, *n*-Bu₄N⁺PF₆⁻ as supporting electrolyte, and a Ag/AgCl electrode as a reference. An internal ferrocene/ferrocenium couple showed $E_{1/2}$ = +0.395 V. The three compounds exhibit the same reversible one-electron oxidation (ΔE_p = ca. 60 mV at scan rates ranging from 50 to 500 mV/s; the ferrocene/ferrocenium couple gave ΔE_p = 60 mV under the same conditions) at the following $E_{1/2}$ values: –0.12 V (X = Cl); –0.06 V (X = Br); –0.02 V (X = I). The product of this electron-transfer process is the Mo(IV) 16-electron cation [MoCpX₂(PMe₃)₂]⁺, which has been isolated from a chemical oxidation reaction for X = Cl (vide supra). The isolated PF₆⁻ salt of the Mo(IV) material (compound 6) shows a cyclic voltammogram identical with that of compound 1, except that the $E_{1/2}$ value for the Mo(III)/Mo(IV) reversible couple is shifted to –0.17 V. A second irreversible oxidation process takes place at higher potentials [$E_{p,a}$ = 1.18 V (X = Cl), 1.26 V (X = Br), 1.20 V (X = I)]. A comparison of the peak heights suggests that this is also a one-electron process.

Contrary to predictions based on the 18-electron rule, a 1-electron reduction to the hypothetical [MoCpX₂(PMe₃)₂]⁻ species is not facile. An irreversible reductive process is observed at –1.51 V (X = Br) and –1.52 V (X = I), whereas for X = Cl no electrochemical reduction is detected before discharge of the solvent occurs.

(e) Molecular Orbital Calculations. We have carried out Fenske–Hall[11] MO calculations on the model compounds MoCpX₂(PH₃)₂ with the objectives of rationalizing the spin state and the optical and electrochemical properties of compounds 1–3 and 6 and the bond length variations observed on going from 1 to 6. A general MO treatment of piano-stool CpML₄ complexes at the extended-Hückel level is already available in the literature.[22b]

The calculations were performed by idealizing the observed structures to C_s symmetry and averaging all the Mo–C(Cp) and C–C(Cp) distances to a common value, so as to attain a perfect η⁵ ligand. The orientation of the Cp ring was left as observed in the structures (e.g. the mirror plane passes through the chlorine atoms in compound 1 and through the phosphorus atoms in compound 3). We have repeated the calculations for the chloride compound after applying a 90° rotation to the Cp ring, so as to make it perfectly isostructural with the iodide compound. The results do not change, suggesting that there is not strong electronic preference for the orientation of the Cp ring, and the conformational difference between 1 and 3 must be merely the result of packing effects.

The calculations have been first carried out by using the minimum basis set, and then they were repeated by including the

(27) Nardelli, M.; Pelizzi, G.; Predieri, G. *Gazz. Chim. Ital.* **1980**, *110*, 375.
(28) Agaskar, P. A.; Cotton, F. A.; Derringer, D. R.; Powell, G. L.; Root, D. R.; Smith, T. J. *Inorg. Chem.* **1985**, *24*, 2786.
(29) Anderson, S. N.; Hughes, D. L.; Richards, R. L. *Transition Met. Chem. (Weinheim, Ger.)* **1985**, *10*, 29.
(30) Fong, L. K.; Fox, J. R.; Foxman, B. M.; Cooper, N. J. *Inorg. Chem.* **1986**, *25*, 1880.
(31) Pelizzi, G.; Predieri, G. *Gazz. Chim. Ital.* **1982**, *112*, 381.
(32) Cotton, F. A.; Fanwick, P. E.; Fitch, J. W.; Glicksman, H. D.; Walton, R. A. *J. Am. Chem. Soc.* **1979**, *101*, 1752.

(33) (a) Angelici, R. J.; Malone, M. D. *Inorg. Chem.* **1967**, *6*, 1731. (b) Venanzi, L. M. *Chem. Brit.* **1968**, 162. (c) Plastas, H. J.; Stewart, J. M.; Grim, S. O. *J. Am. Chem. Soc.* **1969**, *91*, 4326.
(34) Orpen, A. G.; Connelly, N. G. *J. Chem. Soc., Chem. Commun.* **1985**, 1310.
(35) Adam, V. C.; Gregory, U. A.; Kilbourn, B. T. *J. Chem. Soc., Chem. Commun.* **1970**, 1400.
(36) (a) Manojlovic-Muir, L. *J. Chem. Soc. A* **1971**, 2796. (b) Manojlovic-Muir, L.; Muir, K. W. *J. Chem. Soc., Dalton Trans.* **1972**, 686.
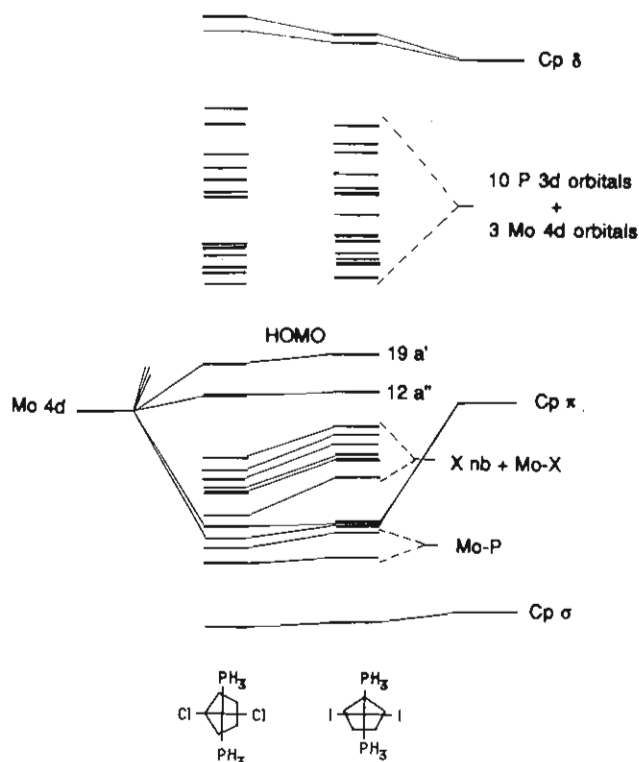
Figure 3. MO diagram for the $MoCpX_2(PH_3)_2$ (X = Cl, I) model compounds. The molybdenum 4d orbitals and the cyclopentadienyl molecular orbitals of π symmetry are drawn at arbitrary energies and are illustrated to emphasize the Mo–Cp σ, π, and δ interactions.

Chart I

19a′   12a″
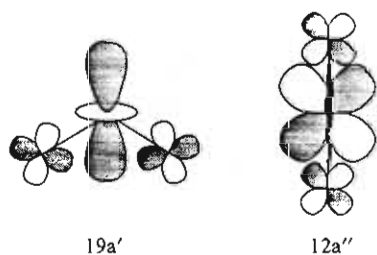
phosphorus 3d atomic functions. The purpose of this second calculation was to test for the possibility of a Mo–P π back-donation. The results of the two different calculations for the same compound do not qualitatively differ except for the relative contributions of atomic orbitals to the HOMO (19a′) and to the second highest occupied MO, or SHOMO (12a″). Figure 3 shows a simplified MO diagram for the two compounds as obtained from the calculations that included the phosphorus 3d orbitals. A complete list of MO energies is available as supplementary material. In brief, the 19a′ orbital has the major contribution from the Mo d_{z^2} orbital (58.7% for X = Cl, 61.2% for X = I) and a substantial contribution from the phosphorus 3d orbitals. The 12a″ orbital is mainly a Mo d_{xy} orbital (66.5% for X = Cl 62.1% for X = I) and also has a significant contribution from P 3d orbitals. The contribution of the 1s atomic orbitals of the phosphine hydrogen atoms to these two MOs is negligible. These interactions are illustrated in Chart I. Both 19a′ and 12a″ also have a contribution from the halogen atom p(π) orbitals, which is of antibonding character.

The Mo d_{xy} orbital has the right symmetry to engage also in a δ-back-bonding combination with the Cp ring. The 12a″ MO shows a small contribution from the Cp carbon p_z orbitals.

Discussion

We have prepared and characterized the molybdenum(III)–cyclopentadienyl derivatives of formula $MoCpX_2(PMe_3)_2$, where X = Cl, Br, and I. These are stable mononuclear odd-electron species, probably because of the strength of the metal–ligand

bonds, which prevents dimerization and formation of a metal–metal bond. These molecules also exhibit a certain degree of Mo–P π interaction, as shown by the lengthening of the Mo–P bond lengths upon oxidation of the chloride species to the Mo(IV) derivative, $[MoCpCl_2(PMe_3)_2]PF_6$.

The Fenske–Hall molecular orbital calculations suggest that this π interaction involves primarily the P 3d orbitals. One of the reviewers points out that the π-acceptor orbitals in the phosphines might be the P–X σ^* orbitals, as suggested by an analysis of the frontier orbitals in phosphine ligands by Trogler, Ellis, and co-workers.[37] Our calculations do not show major contribution of H 1s orbitals to the 19a′ and 12a′ MOs. However, since our calculations were carried out on the model PH_3 phosphine; it is certainly possible that the participation of the phosphine-based orbitals in the two highest occupied MOs is different in nature with respect to the situation present in the actual PMe_3 complex. Although we cannot rule out the involvement of P–CH_3 σ^* orbitals in the π-back-donation mechanism, we have *experimental* data suggesting that this is probably not the major contribution in our case. We shall use the same argument employed by Orpen and Connelly:[34] if the P–X σ^* orbitals participate significantly in the M–P π bonding, a lengthening of the P–X bond distances should be concomitant with the shortening of the M–P bond distance as the π back-donation becomes more important. This was observed[34] to be the case in several examples of pairs of transition-metal–phosphine complexes differing only in the total number of electrons, e.g. $[Mn(CO)(Ph_2PCH_2CH_2PPh_2)(\eta^5\text{-}C_6H_5Ph)]^{n+}$, $[\{Rh(CO)(PPh_3)\}_2(\eta^5,\eta'^5\text{-fulvalene})]^{n+}$, $[\{Rh(CO)(PPh_3)\}_2\{\mu\text{-}N(tolyl)NN(tolyl)\}_2]^{n+}$, and $[CoCp(PEt_3)_2]^{n+}$ (n = 0, 1 in each case). For our pair of phosphine complexes, $[MoCpCl_2(PMe_3)_2]^{n+}$ (n = 0, 1), on the other hand, no significant P–CH_3 bond shortening accompanies the lengthening of the Mo–P bond distances (see Table VI). We point out here that our structural and theoretical evidence indicates that the oxidation of **1** is largely metal-based.

The MO diagram of Figure 3 clearly explains the low-spin configuration of compounds **1–3**. The energy of the $d_{x^2-y^2}$ orbital is raised by σ interaction with the halo and phosphine ligands, while the energy of the d_{xz} and d_{yz} is raised by the π interaction with the Cp ring. On the other hand, the energy of the d_{z^2} orbital is only slightly modified by the σ^* interaction with the Cp ring, the π^* interaction with the halide ligands, and the π interaction with the phosphine ligands, while the d_{xy} orbital feels only the weak interactions with the phosphorus atoms d orbitals (π), with the halide p orbitals (π^*), and with the Cp ligand (δ). As a consequence, the gap between the HOMO and the LUMO (the latter is in fact a phosphorus 3d orbital) is high and the three metal electrons will be accommodated in a $(12a'')^2(19a')^1$ configuration.

It may at first seem strange that compounds **1–3** are easily and reversibly oxidized to 16-electron Mo(IV) species, whereas it is not possible to obtain the corresponding 18-electron Mo(II) anions. One would have predicted the opposite on the basis of the 18-electron rule. Furthermore, examples of 18-electron Mo(II)–Cp complexes in a four-legged piano-stool geometry are common. These generally contain π-acidic ligands such as CO.

The MO diagram shown in Figure 3 and Chart I help rationalizing these observations. The HOMO has weak Mo–Cp σ^* character, while being slightly bonding with respect to the Mo–P π bonds, and the SHOMO is substantially nonbonding. Therefore, the system prefers to give away an antibonding or nonbonding electron to get oxidized to Mo(IV) rather than to take up an extra electron to get reduced to Mo(II). The high-spin configuration experimentally observed for the Mo(IV) product indicates that the 19a′ and 12a″ orbitals will become close in energy in the oxidized product, and the $(19a')^1(12a'')^1$ configuration is preferred over the low-spin $(12a'')^2$ configuration. During the oxidation process, therefore, an electron is extracted from the 12a″ orbital. In terms of bond lengths, the Mo–P distances lengthen partly because of the loss of the 12a″ electron, which is slightly Mo–P

(37) Xiao, S.-X.; Trogler, W. C.; Ellis, D. E.; Berkovitch-Yellin, Z. *J. Am. Chem. Soc.* **1983**, *105*, 7033.

π bonding, but the increase of oxidation state probably plays the major role, because the oxidation process will lower the molybdenum atomic orbital energies, making the Mo–P π bonding (both in 12a″ and in 19a′) less effective. This effect will be, of course, partly compensated by the expected strengthening of the Mo–P σ bonds. The Mo–Cp separation, on the other hand, is not expected to decrease significantly in the oxidation process because the weakly antibonding 19a′ electron is still present in the oxidized material. Instead, an electron is removed from the 12a″ orbital, which is, if anything, weakly δ bonding with respect to the Mo–Cp interaction. The observed slight lengthening of the Mo–C distances on going from **1** to **6** (see Table VI) would seem to indicate that this δ-bonding component has some importance. We observe here that the tilting of the Cp ring toward a η^3,η^2 configuration with the η^2 system *closer* to the metal is also in agreement with a Mo–Cp δ bonding.²²ᵇ Upon oxidation of compound **1** to compound **6**, an electron is lost from the Mo–Cp 12a″ orbital, the δ bonding decreases, and the Cp ligand rearranges to a regular η^5 conformation.

The situation changes if better π-acidic ligands are present. With a stronger π acceptor such as CO the interactions illustrated in Chart I will be much stronger and the energy of the two highest occupied MOs will be substantially lowered. The system will then prefer to accept one more electron to attain the closed-shell 18-electron configuration and maximize the Mo–CO π interactions, while slightly sacrificing the Mo–Cp σ stabilization.

The last point to be addressed concerns the optical properties of compounds **1–3** and **6**. For **1–3**, a separation of 1.47 eV (X = Cl) or 1.52 eV (X = I) is calculated between the $(12a'')^2(19a')^1$ ground state, of type ²A′, and the first excited state $[(12a'')^1-(19a')^2]$, of type ²A″. This corresponds to a photon of wavelength 843 nm (X = Cl) or 816 nm (X = I). We do not observe absorption bands in the visible/near-IR region up to 900 nm, which is the capability of our instrumentation. For compound **6**, a theoretical calculation by the Fenske–Hall method would not have significance because the correlation effects in the observed high-spin configuration would not be treated satisfactorily. However, we can predict that if the molecular orbitals found in the parent Mo(III) molecules maintain their qualitative order in the oxidized species, compound **6** should have as its first excited states the $(12a'')^2$ configuration (of type ¹A′) and the $(19a')^2$ configuration (also ¹A′), as compared with the $(12a'')^1(19a')^1$ ground state (³A″). Two spin-forbidden transitions would therefore be expected at low energy. The UV/visible spectrum of **6** shows two bands of low intensity at 323 nm (ϵ = 935) and 474 nm (ϵ = 1095). It is tempting to assign these two bands to the above-mentioned spin-forbidden transitions, but a more detailed investigation is necessary before a definite assignment can be made.

Conclusions. It appears that the presence of a cyclopentadienyl group is important for providing the molybdenum(III) center with a high degree of π-back-donation ability. An interesting observation in this context is that the only isolated Mo(III)–CO adducts that we are aware of are Cp-containing products, that is $[Mo_2Cp_2(\mu\text{-}SMe)_3(CO)_2]^+X$ (X = Cl, Br, BF₄, PF₆),³ and even CO-containing Mo(IV)–Cp derivatives, namely MoCpX₃(CO)₂ (X = Cl, Br, I), have been described.³⁸ In addition, cyclopentadienyl derivatives of the heavier group 6 metal, tungsten, in relatively high oxidation states have been shown to bind dinitrogen.³⁹

The Fenske–Hall calculations on the model compounds MoCpX₂(PH₃)₂ (X = Cl, I) rationalize a number of experimental observations, such as the spin state of the parent Mo(III) compounds and of the oxidized Mo(IV) species, the electrochemical behavior, and the variation of bond lengths upon oxidation of **1** to **6**. Compound **6** represents a rare example of stable 16-electron molecule in a four-legged piano-stool geometry. Studies on similar derivatives as well as reactivity studies on compounds **1–3** are now in progress in our laboratory.

(38) (a) Haines, R. J.; Nyholm, R. S.; Stiddard, M. H. B. *J. Chem. Soc. A* **1966**, 1606. (b) Green, M. L. H.; Lindsell, W. E. *J. Chem. Soc. A* **1967**, 686.
(39) Murray, R. C.; Schrock, R. R. *J. Am. Chem. Soc.* **1985**, *107*, 4557.